

## Electrocatalysis

International Edition: DOI: 10.1002/anie.201708484  
German Edition: DOI: 10.1002/ange.201708484

## Experimental Proof of the Bifunctional Mechanism for the Hydrogen Oxidation in Alkaline Media

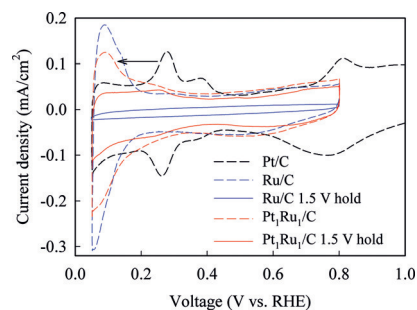
Jingkun Li, Shraboni Ghoshal, Michael K. Bates, Todd E Miller, Veronica Davies, Eli Stavitski, Klaus Attenkofer, Sanjeev Mukerjee, Zi-Feng Ma,\* and Qingying Jia\*

**Abstract:** Realization of the hydrogen economy relies on effective hydrogen production, storage, and utilization. The slow kinetics of hydrogen evolution and oxidation reaction (HER/HOR) in alkaline media limits many practical applications involving hydrogen generation and utilization, and how to overcome this fundamental limitation remains debatable. Here we present a kinetic study of the HOR on representative catalytic systems in alkaline media. Electrochemical measurements show that the HOR rate of Pt-Ru/C and Ru/C systems is decoupled to their hydrogen binding energy (HBE), challenging the current prevailing HBE mechanism. The alternative bifunctional mechanism is verified by combined electrochemical and in situ spectroscopic data, which provide convincing evidence for the presence of hydroxy groups on surface Ru sites in the HOR potential region and its key role in promoting the rate-determining Volmer step. The conclusion presents important references for design and selection of HOR catalysts.

The slow rate of the hydrogen oxidation reaction (HOR) at high pH environment offsets recent advancements in alkaline membranes with applications to alkaline fuel cells and electrolyzers.<sup>[1]</sup> Beyond the practical importance, it is also a most fundamental conundrum in electrochemistry. Markov et al.<sup>[2]</sup> pioneered the fundamental HOR studies aiming to address this long-standing puzzle. They proposed that the HOR kinetics in alkaline is limited by the Volmer step  $M\text{-H}_{\text{ads}} + \text{OH}^- \rightarrow M + \text{H}_2\text{O} + e^-$ , and the reactive hydroxy species ( $\text{OH}_{\text{ads}}$ ) is required to promote this step. Accordingly, a three dimensional volcano plot was proposed wherein the HOR rate is co-determined by the binding of the hydrogen intermediate ( $\text{H}_{\text{ads}}$ ), as well as of the  $\text{OH}_{\text{ads}}$  to the surface.<sup>[3]</sup>

The enhanced HOR activity of Pt in alkaline by decorating it with  $\text{Ni}(\text{OH})_2$  adislands or alloying it with Ru was accordingly attributed to the incorporation of surface oxophilic sites accommodating reactive  $\text{OH}_{\text{ads}}$ . This mechanism is however undermined by the lack of experimental evidence for the reactive  $\text{OH}_{\text{ads}}$  species in the HOR potential region. The current prevailing theory for the HOR kinetics is the so-called hydrogen binding energy (HBE) mechanism, wherein the HOR rate of a variety of mono-metallic surfaces (Pt, Ir, Pd, and Rh) with various facets over a broad pH range (0 to 13) is solely determined by the HBE ( $E_{\text{M-H}}$ ).<sup>[4]</sup> The HBE mechanism was also applied to account for the superior HOR activity of Pt-Ru systems to Pt.<sup>[5]</sup> The great success of this mechanism lies in not only the generality, but also the verifiability that the HOR rate of a broad range of catalytic surfaces can be directly related to  $E_{\text{M-H}}$  via the position of the underpotential deposited hydrogen  $\text{H}_{\text{UPD}}$  stripping peak ( $E_{\text{peak}}$ ) ( $E_{\text{M-H}} = -E_{\text{peak}}F$  where  $F$  is the Faraday constant).<sup>[4d,5c]</sup> For instance, the superior HOR activity of the PtRu alloy to that of Pt was ascribed to the Ru-induced weakening of the  $E_{\text{Pt-H}}$  as reflected by the more negative  $\text{H}_{\text{UPD}}$  stripping peak position (Figure 1).<sup>[5c]</sup> However, we noticed that the  $\text{H}_{\text{UPD}}$  peak of the  $\text{Pt}_1\text{Ru}_1/\text{C}$  alloy (ETEK, 29.1 wt %) largely overlapped that of Ru/C (ETEK, 60 wt %) (Figure 1). This observation implicated that this  $\text{H}_{\text{UPD}}$  peak may arise from the surface Ru rather than Pt sites. By demonstrating this is indeed the case as a starting point, herein we discarded the HBE mechanism by decoupling the  $E_{\text{M-H}}$  of Pt-Ru and Ru systems to their HOR rate, and verified the alternative  $\text{OH}_{\text{ads}}$ -induced bifunctional mechanism by experimentally identifying the presence of  $\text{OH}_{\text{ads}}$  in the HOR potential region and its promoting role on the HOR kinetics in alkaline media.

[\*] J. Li, S. Ghoshal, M. K. Bates, T. E. Miller, V. Davies, S. Mukerjee, Q. Jia

Department of Chemistry and Chemical Biology  
Northeastern University, Boston, MA 02115 (USA)  
E-mail: q.jia@neu.eduE. Stavitski, K. Attenkofer  
National Synchrotron Light Source II  
Brookhaven National Laboratory  
Upton, NY 11973 (USA)Z.-F. Ma  
Shanghai Electrochemical Energy Devices Research Center  
Department of Chemical Engineering  
Shanghai Jiao Tong University  
Shanghai 200240 (China)  
E-mail: zfma@sjtu.edu.cnSupporting information and the ORCID identification number(s) for the author(s) of this article can be found under:  
<https://doi.org/10.1002/anie.201708484>

**Figure 1.** CV plots of Pt/C, Ru/C, and  $\text{Pt}_1\text{Ru}_1/\text{C}$ ; and of the latter two after holding the potential at 1.5 V for 5 minutes. All CVs plots were collected in an Ar-saturated 0.1 M KOH electrolyte at a scan rate of  $20 \text{ mV s}^{-1}$  at room temperature. The loading of Pt for Pt/C and  $\text{Pt}_1\text{Ru}_1/\text{C}$ , and of Ru for Ru/C is ca.  $10 \mu\text{g cm}_{\text{disk}}^{-2}$ .

Since the  $H_{\text{UPD}}$  stripping on Ru/C occurs on the metallic Ru sites,<sup>[6]</sup> we inferred that the  $H_{\text{UPD}}$  peak would diminish by irreversible formation of oxides on Ru surfaces. Accordingly, we held the Ru/C at 1.5 V (all potentials reported here were vs. reversible hydrogen electrode, RHE) for five minutes to irreversibly oxidize the surface Ru. The subsequent cyclic voltammetry (CV) starting directly at 0.05 V was featureless due to the dissolution and passivation of the surface Ru (Figure 1).<sup>[7]</sup> The same process was then applied to Pt<sub>1</sub>Ru<sub>1</sub>/C. The  $H_{\text{UPD}}$  peak around 0.1 V disappeared, accompanied with the emergence of the  $H_{\text{UPD}}$  peak around 0.27 V (Figure 1). These results indicated that the  $H_{\text{UPD}}$  peak of Pt<sub>1</sub>Ru<sub>1</sub>/C around 0.1 V arises from Ru rather than Pt as assumed previously,<sup>[5c]</sup> and the  $E_{\text{Pt-H}}$  in the Pt<sub>1</sub>Ru<sub>1</sub>/C alloy is not significantly altered, thereby calling in question the HBE mechanism on the Pt-Ru alloy that rests on the erroneous assignment of the  $H_{\text{UPD}}$  peak.<sup>[5c]</sup>

The above results suggested that the Pt-Ru alloying phase was not required to improve the HOR kinetics of Pt in alkaline, whereas the presence of surface Ru was essential. Based on this deduction, surface electrochemical deposition of Ru on Pt/C was applied to introduce surface Ru to explore its role on the HOR kinetics and the  $H_{\text{UPD}}$  peak position. The feasibility of this method is justified by the fact that Ru can be spontaneously deposited on platinum and remains stable within a wide potential range.<sup>[8]</sup> Specifically, the HOR performance of Pt/C (46.7%, TKK) was assessed on a rotating disk electrode (RDE) in 0.1 M KOH as a baseline (Figure 2 a).

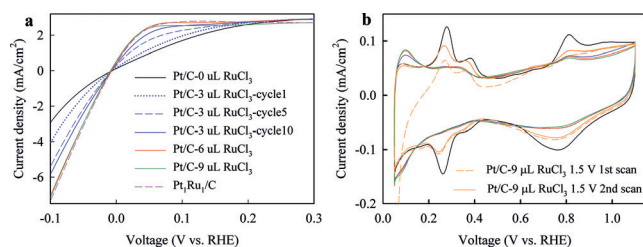


**Figure 2.** a) HOR polarization curves of Pt/C with 0, 3, 6, and 9  $\mu\text{L}$  doped 5 mM  $\text{RuCl}_3$  and Pt<sub>1</sub>Ru<sub>1</sub>/C collected in a  $\text{H}_2$ -saturated 0.1 M KOH electrolyte at a scan rate of  $10 \text{ mV s}^{-1}$  and a rotation rate of 2500 rpm at room temperature. b) Cyclic voltammograms of Pt/C with 0, 3, 6, and 9  $\mu\text{L}$  doped 5 mM  $\text{RuCl}_3$  and the latest case after holding at 1.5 V for 5 minutes collected in an Ar-saturated 0.1 M KOH electrolyte at  $20 \text{ mV s}^{-1}$ . The Pt loading is ca.  $10 \mu\text{g cm}_{\text{disk}}^{-2}$ .

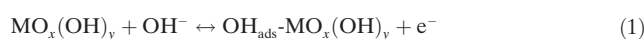
This was followed by doping with 3  $\mu\text{L}$  5 mM  $\text{RuCl}_3$  solution into the electrolyte (corresponding to  $0.5 \mu\text{M Ru}^{3+}$ ) without applying potentials. The subsequent HOR tests showed a gradual increase in the HOR rate with voltage cycling until reaching a stable state (Figure 2 a). The HOR rate was further improved by doping with another 3  $\mu\text{L}$   $\text{RuCl}_3$ , approaching that of Pt<sub>1</sub>Ru<sub>1</sub>/C. These results demonstrated that the surface doped Ru improves the HOR rate of Pt/C in alkaline.

The CV was recorded after each HOR testing to trace the Ru-induced shift of the  $H_{\text{UPD}}$  peak. The  $H_{\text{UPD}}$  peak around 0.1 V overlapping that of Pt<sub>1</sub>Ru<sub>1</sub>/C and Ru/C emerged upon the doping of 3  $\mu\text{L}$   $\text{RuCl}_3$  (Figure 2 b). We then held the Pt/C

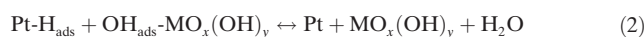
electrode with 9  $\mu\text{L}$  doped  $\text{RuCl}_3$  at 1.5 V for 5 minutes. In the subsequent CV starting at 0.05 V, the  $H_{\text{UPD}}$  peak at 0.1 V again disappeared, which was accompanied by the reemergence of the prominent  $H_{\text{UPD}}$  peak at 0.27 V associated with the  $H_{\text{UPD}}$  peak of the Pt (110) facet. These observations are consistent with those obtained on the Pt<sub>1</sub>Ru<sub>1</sub>/C alloy, providing conclusive evidence that their superior HOR kinetics is not governed by the Ru-induced change of the  $E_{\text{Pt-H}}$ , thereby revoking the HBE mechanism for the superior HOR kinetics of Pt-Ru systems.

The notion that the HBE mechanism accounts for the superior HOR kinetics of Pt-Ru systems is based on not only the “shift” of the  $H_{\text{UPD}}$  peak,<sup>[5c]</sup> but also the observation that Ru@Pt core-shell nanoparticles (NPs) with pure Pt surfaces exhibit improved HOR kinetics compared to Pt/C NPs.<sup>[5a,b]</sup> This remark, however, merits another look. An important implication of the doped Ru experiment is that even trace amount of Ru ( $0.5 \mu\text{M}$ ) in the electrolyte can significantly boost the HOR of Pt/C in alkaline. This finding raises the question whether the clean Pt surfaces characterized under ex situ conditions are really free of Ru under in situ electrochemical conditions where the HOR kinetics is assessed, especially considering that Ru can migrate onto the Pt surfaces<sup>[9]</sup> and then gets dissolved into electrolyte upon voltage cycling.<sup>[6]</sup> Indeed, the CV of the Ru@Pt NPs clearly exhibits a  $H_{\text{UPD}}$  peak at 0.1 V in alkaline, indicating the presence of surface Ru.<sup>[5a]</sup> The absence of the broad peak associated with the reduction of  $\text{Ru}(\text{OH})_x$  of Ru@Pt NPs was proposed as the in situ evidence for the pure Pt surface free of Ru, but it was conducted under acidic media, and the CV in alkaline was not reported.<sup>[5b]</sup>

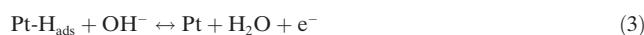
Since the new evidences obtained on Pt-Ru systems underscore the essential role of surface oxophilic metal hydr(oxy)oxides for the superior HOR kinetics, we turned to examine the bifunctional mechanism<sup>[2]</sup> wherein the reactive  $\text{OH}_{\text{ads}}$  accommodated by metal hydr(oxy)oxides [Eq. (1)]



facilitates the oxidation of  $\text{H}_{\text{ads}}$  on adjacent Pt sites [Eq. (2)],



thereby promoting the Volmer step [Eq. (3)]:



The bane of this mechanism lies in the lack of unambiguous evidence for the reactive  $\text{OH}_{\text{ads}}$  at low potentials. For instance, Zhuang et al.<sup>[5c]</sup> questioned this mechanism by showing that the presence of reactive  $\text{OH}_{\text{ads}}$  species on the surface of Pt-Ru/C at the HOR potential region is not supported by the CO stripping experiment. However, the Pt-Ru/C alloy is subject to the so-called pseudo-bifunctional mechanism for CO oxidation, wherein the Ru sites are also occupied by  $\text{CO}_{\text{ads}}$  below 0.4 V (e.g. the HOR potential region), and only get oxidized by the site competitor  $\text{OH}_{\text{ads}}$  at potentials above 0.4 V (see Figure S1 in the Supporting Information).<sup>[10]</sup> Therefore, the absence of the CO stripping

peak of the Pt-Ru/C alloy below 0.4 V by no means indicate the absence of  $\text{OH}_{\text{ads}}$  at the HOR conditions, under which no  $\text{CO}_{\text{ads}}$  competes over the Ru sites with  $\text{OH}_{\text{ads}}$ . In order to possibly see the reactive  $\text{OH}_{\text{ads}}$  via CO stripping, the surface Ru sites must not be fully occupied by  $\text{CO}_{\text{ads}}$  at the HOR potential region, which was realized in the Ru-doped Pt/C system as shown next.

The CO stripping experiment was conducted on the Pt/C with various amount of doped  $\text{RuCl}_3$ . The intensity of the CO stripping peak at 0.7 V gradually decreased with increasing amount of doped  $\text{RuCl}_3$  (Figure 3), indicating the

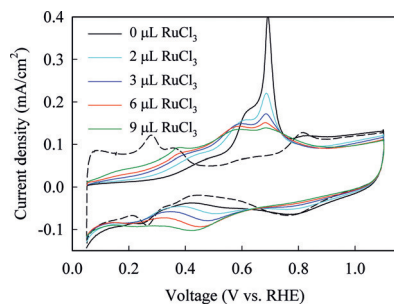


**Figure 3.** CO stripping voltammograms collected for Pt/C with various amount of deposited  $\text{RuCl}_3$  in Ar-saturated 0.1 M KOH at a scan rate of  $20 \text{ mV s}^{-1}$ .

reduced amount of unperturbed Pt sites. This was accompanied by the gradual increase of the intensity of the CO stripping peak starting as low as 0.05 V, which was ascribable to the increased population of the Pt sites with the CO oxidation promoted by adjacent Ru. The emergence of two CO oxidation peaks agrees with the kinetic model by Koper et al.<sup>[11]</sup> based on the Ru-induced local bifunctional effect that requires large Ru islands on the Pt surface and low CO mobility. The results clearly showed that some doped Ru sites can accommodate reactive  $\text{OH}_{\text{ads}}$  at potentials below 0.4 V, rather than predominately occupied by  $\text{CO}_{\text{ads}}$  like the Pt-Ru/C alloy. This was supported by the redox features of Ru slightly below 0.4 V (Figure 3) that was absent for  $\text{Pt}_1\text{Ru}_1/\text{C}$  and Ru/C (Figure S1). This observation is in accordance with the previous finding<sup>[12]</sup> of Markovic et al. that the electrodeposited transition metal hydr(oxy)oxides on Pt(111) preferentially binds  $\text{OH}_{\text{ads}}$ ,<sup>[10,12b]</sup> resulting in early CO oxidation.

Likewise, the presence of unperturbed Pt and Ru-promoted Pt sites in the Ru-doped Pt/C for the HOR was reflected by the two distinct trends in the micropolarization region of the HOR curves, or in the corresponding Tafel plots (Figure 4). With increasing amount of doped Ru, the HOR kinetics below 0.2 V was improved, and the Tafel slope gradually decreased from that of Pt/C (ca. 135 mV/dec) to that of  $\text{Pt}_1\text{Ru}_1/\text{C}$  (Figure 4b); whereas the HOR kinetics above  $\approx 0.2 \text{ V}$  remained unchanged. The evolution of the Tafel slope suggested that the doped Ru changed the rate determining step (rds) of the adjacent Pt sites from the Volmer step involving an electron transfer, probably to the Tafel step without electron transfer. Increasing the amount of doped  $\text{RuCl}_3$  from 6 to 9  $\mu\text{L}$  did not change the HOR kinetics, but led to the reduction of the limiting current density

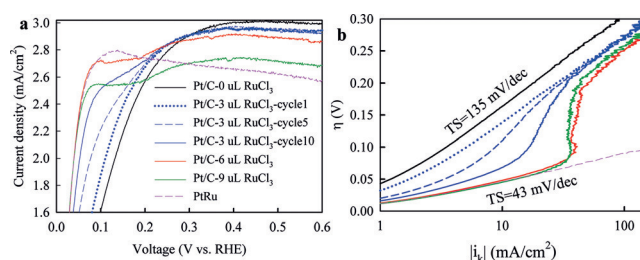


**Figure 4.** a) Reproduced from Figure 2a focusing on the HOR kinetic region; b) the corresponding kinetic plots. The “slope” of  $\text{Pt}_1\text{Ru}_1/\text{C}$  is given only for comparison purposes as its HOR rate is limited by the mass diffusion of  $\text{H}_2$ .

(Figure 4a). This indicated that the primary active site for the HOR is Pt rather than Ru, otherwise the opposite trend would be observed. Therefore the change of the rds cannot be ascribed to the change of active site, but rather to the reactive  $\text{OH}_{\text{ads}}$  accommodated by Ru that promotes the Volmer step via the bifunctional mechanism [Eq. (2)], just like it promoting the CO oxidation (Figure 3). The local bifunctional effect was absent on  $\text{Pt}_1\text{Ru}_1/\text{C}$  (Figure 4b and Figure S1a) owing to the uniform distribution of surface Ru.<sup>[11]</sup> Despite the different surface morphology between the Ru-doped Pt/C and  $\text{Pt}_1\text{Ru}_1/\text{C}$ , their identical HOR kinetics below 0.2 V (Figure 4b) suggested that their superior HOR kinetics was governed by the same underlying mechanism.

To directly observe the reactive  $\text{OH}_{\text{ads}}$  at the HOR potential region, we conducted in situ XAS on  $\text{Pt}_1\text{Ru}_1/\text{C}$ , Pt/C, and Ru/C. As seen in Figure 5, the X-ray absorption near edge structure (XANES) of the Ru K-edge spectra for both Ru/C and  $\text{Pt}_1\text{Ru}_1/\text{C}$  shifts to higher energy as the potential increases from 0.05 to 0.24 V. The derived  $\Delta\mu$  matches the theoretical  $\Delta\mu$  obtained by the ab initio FEFF calculations<sup>[13]</sup> by replacing the  $\text{H}_{\text{ads}}$  on the  $\text{Ru}_6$  cluster model by  $\text{OH}_{\text{ads}}$ . The replacement of  $\text{H}_{\text{ads}}$  by  $\text{OH}_{\text{ads}}$  on Ru sites in the HOR region is also reflected by the sharpness of the  $\text{H}_{\text{UPD}}$  peak associated with attractive lateral interactions.<sup>[14]</sup> The replacement ends around 0.2 V as previously proposed,<sup>[15]</sup> followed by the formation of amorphous layers of  $\text{Ru}(\text{OH})_3$  around 0.2 V in 0.1 M KOH.<sup>[7]</sup> The formation of  $\text{Ru}(\text{OH})_3$  at 0.2 V is further supported by the observation that the HOR curves of Ru/C drops around 0.2 V (Figure S2a), which was previously observed<sup>[2,16]</sup> and ascribed to the formation of hydr(oxy)oxides that block active sites.<sup>[2]</sup> The combined XAS and electrochemical data provide substantial evidence for the dynamic co-existence of  $\text{H}_{\text{ads}}$  and  $\text{OH}_{\text{ads}}$  on Ru sites at the HOR region. This observation is in line with the well-known phenomenon of the co-existence of  $\text{H}_{\text{ads}}$  and  $\text{OH}_{\text{ads}}$  on a Ru(0001) surface in vacuum as a result of the partial water dissociation.<sup>[17]</sup>

The promoting role of the  $\text{OH}_{\text{ads}}$  for the Volmer step of Pt-Ru systems via facilitating the oxidation of  $\text{H}_{\text{ads}}$  on Pt sites [Eq. (3)] is confirmed by the XANES spectra collected at the Pt  $L_{3-}$  edge of  $\text{Pt}_1\text{Ru}_1/\text{C}$  and Pt/C. The Pt white line intensity of Pt/C remains unchanged in the potential region of 0.05–0.24 V, and is lower than that at 0.54 V (double layer region) (Figure 5c and d) due to the adsorption of H onto the Pt fcc sites,<sup>[18]</sup> which was confirmed by the surface sensitive  $\Delta\mu$ -

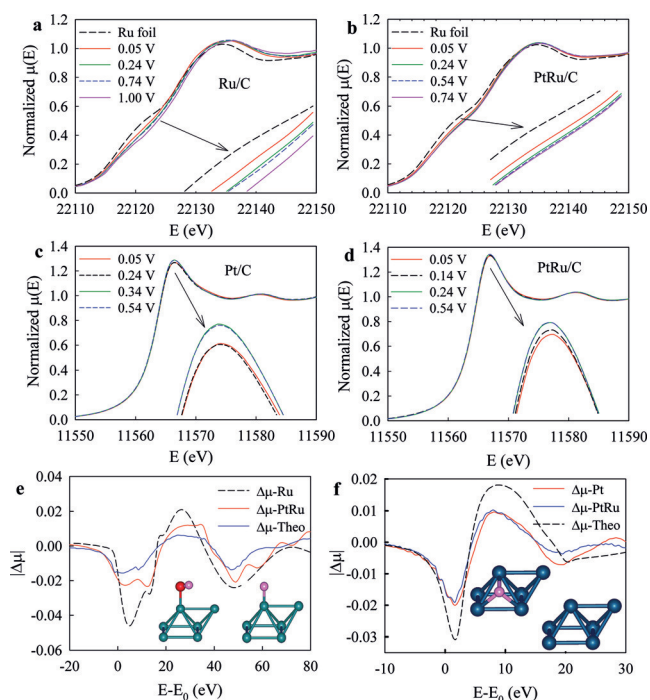


**Figure 5.** Ru K-edge XANES spectra of Ru/C (a) and Pt<sub>1</sub>Ru<sub>1</sub>/C (b); and the Pt L<sub>3</sub>-edge XANES spectra of Pt/C (c) and Pt<sub>1</sub>Ru<sub>1</sub>/C (d) collected in H<sub>2</sub>-saturated 0.1 M KOH at various potentials. e) Experimental  $\Delta\mu$  signals derived from the XANES spectra displayed in (a) and (b) ( $\Delta\mu = \mu(0.24 \text{ V}) - \mu(0.05 \text{ V})$ ), and the theoretical  $\Delta\mu$  ( $\Delta\mu\text{-Theo} = \mu(\text{Ru}_6\text{-OH}) - \mu(\text{Ru}_6\text{-H})$ ) with the model clusters given in the inset. f) Experimental  $\Delta\mu$  signals derived from the XANES spectra displayed in (c) and (d) ( $\Delta\mu = \mu(0.05 \text{ V}) - \mu(0.54 \text{ V})$ ), and the theoretical  $\Delta\mu$  ( $\Delta\mu\text{-Theo} = \mu(\text{Pt}_6\text{-H}) - \mu(\text{Pt}_6)$ ) with the model clusters given in the inset. The green, blue, red, and pink balls represent Ru, Pt, O, and H atoms, respectively.

XANES analysis (Figure 5 f). The white line intensity of Pt/C increases mostly between 0.24 and 0.34 V (Figure 5 c), indicating the primary desorption of H<sub>ads</sub> in this potential region, matching the prominent H<sub>UPD</sub> stripping peak of Pt/C around 0.27 V (Figure 1). In contrast, the Pt white line intensity of Pt<sub>1</sub>Ru<sub>1</sub>/C gradually increases with potential from 0.05 V to 0.24 V, and remains unchanged in the potential range of 0.24–0.54 V. This indicates that the majority of the H<sub>ads</sub> leaves the surface Pt sites of Pt<sub>1</sub>Ru<sub>1</sub>/C below 0.24 V. While this cannot be directly observed in the cyclic voltammograms since the H<sub>UPD</sub> stripping peak from Ru dominates in this potential region, it is reflected by the absence of the H<sub>UPD</sub> peak at 0.27 V of Pt<sub>1</sub>Ru<sub>1</sub>/C (Figure 1), and of Pt/C with surface deposited Ru (Figure 2b). The observations of reactive OH<sub>ads</sub> on Ru sites and the facilitated H desorption from Pt surfaces at the HOR potential region provide experimental evidence for the bifunctional mechanism.

While the bifunctional mechanism is established on bimetallic systems, it is also applicable to certain monometallic systems such as Ru (experimental verification given in the Supporting Information section 2.2) since the XANES and electrochemical data clearly showed the OH<sub>ads</sub>-facilitated oxidation of H<sub>ads</sub> on the surface of Ru/C. Ru/C also exhibits high HER activity in alkaline (see Figure S2a and Figure S4).

In addition, the HER of Pt/C in alkaline is also improved by surface Ru (Figure 2a), which agrees with previous findings that oxophilic metal hydr(oxy)oxides on the Pt surface promote the Volmer step of the HER, the reverse of the HOR.<sup>[12,19]</sup> The combined HER/HOR results strongly suggest that oxophilic metal hydr(oxy)oxides lowers the energy barrier of the Volmer step via the bifunctional mechanism, and thereby improves the HOR/HER kinetics simultaneously (note other factors induced by oxophilic metal hydr(oxy)oxides may also affect the HER kinetics,<sup>[20]</sup> but it is beyond the scope of this work).

In summary, we provided the first experimental evidence for the presence of OH<sub>ads</sub> on the surface Ru sites in the HOR potential region and its promoting effect on the oxidation of H<sub>ads</sub> for both Pt-Ru/C and Ru/C systems, thereby verifying the bifunctional mechanism for the HOR in alkaline. The clarification of the governing mechanism for the HOR kinetics in alkaline media is essential for the development of HOR catalysts.

## Acknowledgements

Current financial support from ARPA-E lead by Pajarito Powders is deeply appreciated. This work was also supported by the Natural Science Foundation of China (21676165, 21336003). Use of Beamline 2-2 of the Stanford Synchrotron Radiation Lightsource (SSRL), SLAC National Accelerator Laboratory, is supported by the U.S. Department of Energy, Office of Science, Office of Basic Energy Sciences under contract number DE-AC02-76SF00515. Use of Beamline ISS 8-ID of the NSLS II was supported by the National Synchrotron Light Source (NSLS) II, Brookhaven National Laboratory, under U.S. DOE contract number DE-SC0012704.

## Conflict of interest

The authors declare no conflict of interest.

**Keywords:** alloys · electrocatalysis · electrochemistry · reaction mechanisms · supported catalysts

**How to cite:** *Angew. Chem. Int. Ed.* **2017**, *56*, 15594–15598  
*Angew. Chem.* **2017**, *129*, 15800–15804

- [1] a) G. Merle, M. Wessling, K. Nijmeijer, *J. Membr. Sci.* **2011**, *377*, 1–35; b) J. Pan, C. Chen, Y. Li, L. Wang, L. Tan, G. Li, X. Tang, L. Xiao, J. Lu, L. Zhuang, *Energy Environ. Sci.* **2014**, *7*, 354–360.
- [2] D. Strmcnik, M. Uchimura, C. Wang, R. Subbaraman, N. Danilovic, D. van der Vliet, A. P. Paulikas, V. R. Stamenkovic, N. M. Markovic, *Nat. Chem.* **2013**, *5*, 300–306.
- [3] M. T. Koper, *Nat. Chem.* **2013**, *5*, 255–256.
- [4] a) J. Durst, A. Siebel, C. Simon, F. Hasche, J. Herranz, H. A. Gasteiger, *Energy Environ. Sci.* **2014**, *7*, 2255–2260; b) W. Sheng, H. A. Gasteiger, Y. Shao-Horn, *J. Electrochem. Soc.* **2010**, *157*, B1529–B1536; c) J. Zheng, W. Sheng, Z. Zhuang, B. Xu, Y. Yan, *Sci. Adv.* **2016**, *2*, e1501602; d) W. Sheng, Z. Zhuang, M. Gao, J. Zheng, J. G. Chen, Y. Yan, *Nat. Commun.* **2015**, *6*, 5848.

- [5] a) K. Elbert, J. Hu, Z. Ma, Y. Zhang, G. Chen, W. An, P. Liu, H. S. Isaacs, R. R. Adzic, J. X. Wang, *ACS Catal.* **2015**, *5*, 6764–6772; b) J. N. Schwämmlein, H. A. El-Sayed, B. M. Stühmeier, K. F. Wagenbauer, H. Dietz, H. A. Gasteiger, *ECS Trans.* **2016**, *75*, 971–982; c) Y. Wang, G. Wang, G. Li, B. Huang, J. Pan, Q. Liu, J. Han, L. Xiao, J. Lu, L. Zhuang, *Energy Environ. Sci.* **2015**, *8*, 177–181.
- [6] Y. Sugawara, A. Yadav, A. Nishikata, T. Tsuru, *J. Electrochem. Soc.* **2008**, *155*, B897–B902.
- [7] J. Juodkazytė, R. Vilkauskaitė, B. Šebeka, K. Juodkazis, *Trans. IMF* **2007**, *85*, 194–201.
- [8] W. Chrzanowski, A. Wieckowski, *Langmuir* **1997**, *13*, 5974–5978.
- [9] B. Han, A. Van der Ven, G. Ceder, B.-J. Hwang, *Phys. Rev. B* **2005**, *72*, 205409.
- [10] N. M. Marković, P. N. Ross, *Surf. Sci. Rep.* **2002**, *45*, 117–229.
- [11] M. Koper, J. Lukkien, A. Jansen, R. Van Santen, *J. Phys. Chem. B* **1999**, *103*, 5522–5529.
- [12] a) R. Subbaraman, D. Tripkovic, D. Strmcnik, K.-C. Chang, M. Uchimura, A. P. Paulikas, V. Stamenkovic, N. M. Markovic, *Science* **2011**, *334*, 1256–1260; b) R. Subbaraman, D. Tripkovic, K.-C. Chang, D. Strmcnik, A. P. Paulikas, P. Hirunsit, M. Chan, J. Greeley, V. Stamenkovic, N. M. Markovic, *Nat. Mater.* **2012**, *11*, 550–557.
- [13] J. J. Rehr, J. J. Kas, M. P. Prange, A. P. Sorini, Y. Takimoto, F. Vila, *C. R. Phys.* **2009**, *10*, 548–559.
- [14] a) N. Garcia-Araez, J. J. Lukkien, M. T. M. Koper, J. M. Feliu, *J. Electroanal. Chem.* **2006**, *588*, 1–14; b) M. J. Van der Niet, N. Garcia-Araez, J. Hernández, J. M. Feliu, M. T. Koper, *Catal. Today* **2013**, *202*, 105–113.
- [15] D. Michell, D. A. J. Rand, R. Woods, *J. Electroanal. Chem. Interfacial Electrochem.* **1978**, *89*, 11–27.
- [16] J. Ohyama, T. Sato, Y. Yamamoto, S. Arai, A. Satsuma, *J. Am. Chem. Soc.* **2013**, *135*, 8016–8021.
- [17] a) P. J. Feibelman, *Science* **2002**, *295*, 99–102; b) M. Tatarkhanov, E. Fomin, M. Salmeron, K. Andersson, H. Ogasawara, L. G. Pettersson, A. Nilsson, J. Cerdá, *J. Chem. Phys.* **2008**, *129*, 154109.
- [18] a) M. Teliska, W. O'Grady, D. Ramaker, *J. Phys. Chem. B* **2004**, *108*, 2333–2344; b) T. Kubota, K. Asakura, N. Ichikuni, Y. Iwasawa, *Chem. Phys. Lett.* **1996**, *256*, 445–448.
- [19] a) Z. Liang, H. S. Ahn, A. J. Bard, *J. Am. Chem. Soc.* **2017**, *139*, 4854–4858; b) Z. Zeng, K.-C. Chang, J. Kubal, N. M. Markovic, J. Greeley, *Nat. Energy* **2017**, *2*, 17070.
- [20] I. Ledezma-Yanez, W. D. Z. Wallace, P. Sebastián-Pascual, V. Climent, J. M. Feliu, M. T. Koper, *Nat. Energy* **2017**, *2*, 17031.

Manuscript received: August 17, 2017

Revised manuscript received: October 1, 2017

Accepted manuscript online: October 16, 2017

Version of record online: November 8, 2017